

---

Complex and Social Networks  
 Laboratory 5 - Network Dynamics  
 Gabriele Villa & Davide Volpi  
 Academic Year 2025/2026

---

## 1 Introduction

The aim of this laboratory session is to simulate and statistically analyze different network growth models, focusing on the Barabási-Albert (BA) model and its variants.

In this session, we investigate the mathematical properties of the BA model and two modifications: one with random attachment instead of preferential attachment, and another without vertex growth. For each model, we analyze the temporal evolution of vertex degrees and the resulting degree distributions, applying statistical methods and curve fitting techniques to better understand the underlying dynamics and compare the models' behaviours.

## 2 Results

### 2.1 Barabási-Albert with Preferential Attachment

#### 2.1.1 Degree sequence

Initially, from the aggregated degree sequence we constructed the empirical degree distribution

$$\hat{P}(k) = \frac{1}{N} \sum_{i=1}^N \mathbf{1}_{\{k_i=k\}},$$

and compared several candidate parametric models with the AIC.

For the BA model with preferential attachment, the AIC analysis indicates that the best fit for the aggregated final degree distribution is provided by a right-truncated zeta (power-law) distribution with exponent

$$\hat{\gamma} \approx 2.77.$$

This truncated power-law model not only minimizes the AIC among the considered candidates, but also provides a good visual fit to the empirical degree distribution on log-log axes, especially across the intermediate and large-degree region.

Model	AIC	$\Delta$ AIC	Parameters
Zeta Trunc	50265185	0	$\gamma = 2.7698$ , $k_{\max} = 1580$
Zeta	50265789	604	$\gamma = 2.7703$
Zeta ( $\gamma=3$ )	50418767	153582	$\gamma = 3$
Geometric	67026455	16761270	$q = 0.0909$
Geom Trunc	67026457	16761272	$q = 0.0909$ , $k_{\max} = 1580$
Poisson	109111610	58846425	$\lambda = 9.9995$

Table 1: AIC of models for the Barabási-Albert preferential attachment degree distribution.

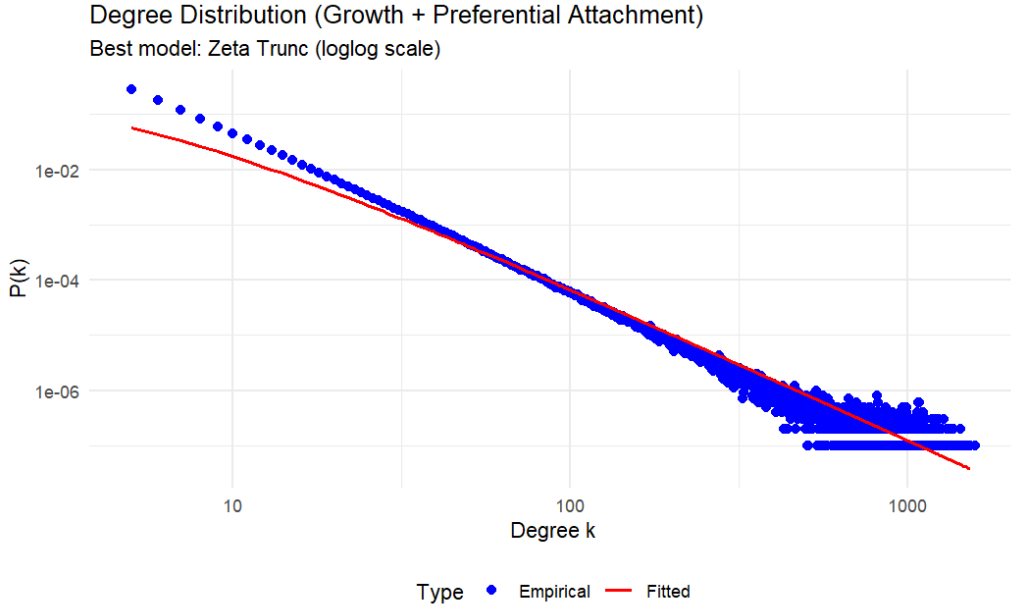


Figure 1: Best degree distribution fit for the BA preferential model

### 2.1.2 Scaling of vertex degree over time

First of all we made a plot that shows the rescaled degree  $k'_i(t)$  obtained by applying the transformation:

$$k'_i(t) = t_i^{1/2} k_i(t) \approx m_0 t^{1/2}$$

This operation was performed to check the theoretical prediction that the rescaled growth rate should be approximately the same for all vertices, regardless of their arrival time  $t_i$ . Furthermore, a log-log scale was used for the plot to effectively display the expected power-law dependency:

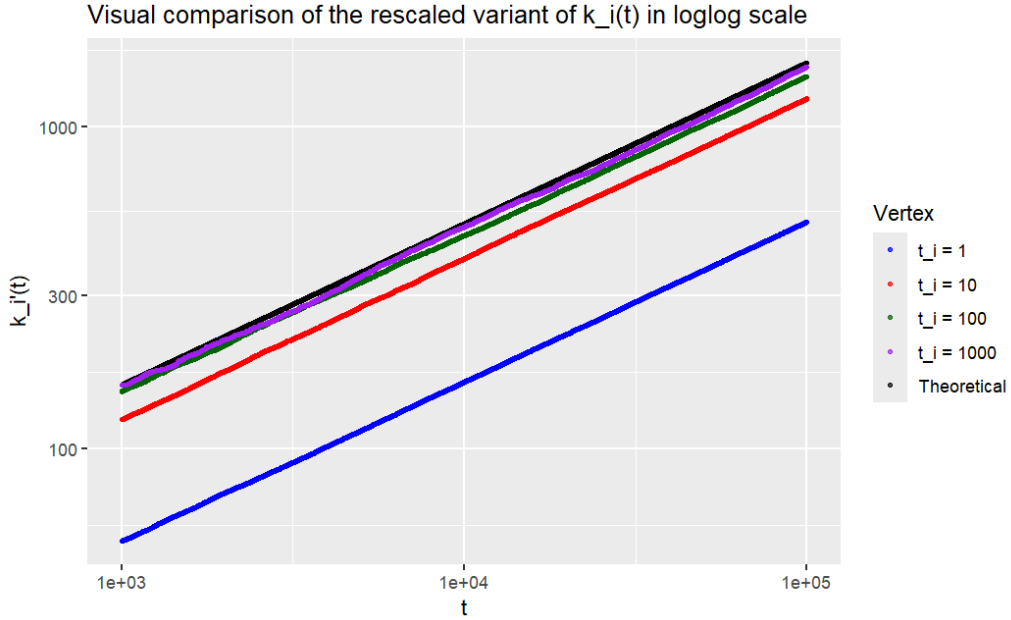


Figure 2: Rescaled variant of degree growth over time for different arrival times

Now we also present the four log-log plots showing the evolution of the degree sequences over time for the vertices that arrived at times  $t = 1$ ,  $t = 10$ ,  $t = 100$ , and  $t = 1000$ .

In each plot, the empirical data are displayed in blue, the theoretical curve in green, and the fitted curve in red. The theoretical curve is given by the expected formula,

$$k_i(t) \approx m_0 \left( \frac{t}{t_i} \right)^{\frac{1}{2}},$$

which we compare against the observed behaviour of the degree sequences. The best fitting model was chosen according to the AIC criterion: for completeness, we also present the values of AIC for each model and for each degree growth.

Model	AIC	$\Delta AIC$
Model 2+	52819.1	0.0
Model 2	54825.9	2006.8
Model 1+	66905.0	14086.0
Model 1	178147.5	125328.4
Model 4+	603763.7	550944.7
Model 0+	919039.8	866220.8
Model 3+	919817.2	866998.1
Model 3	1017772.5	964953.5
Model 0	1139767.2	1086948.1
Model 4	1181748.0	1128929.0

Table 2: AIC of models for the Barabasi Albert preferential algorithm for vertex arriving at t=1

Model	AIC	$\Delta AIC$
Model 2+	104012.7	0.0
Model 2	104243.6	230.9
Model 1+	116723.5	12710.8
Model 1	198541.1	94528.5
Model 4+	563122.4	459109.8
Model 0+	864455.7	760443.0
Model 3+	865232.7	761220.0
Model 3	962775.6	858762.9
Model 0	1086002.5	981989.8
Model 4	1127227.7	1023215.0

Table 3: AIC of models for the Barabasi Albert preferential algorithm for vertex arriving at t=10

Model	AIC	$\Delta AIC$
Model 2+	8950.3	0.0
Model 1+	25410.3	16460.0
Model 2	53000.7	44050.4
Model 1	92921.6	83971.3
Model 4+	357817.1	348866.8
Model 0+	657551.3	648600.9
Model 3+	658371.6	649421.3
Model 3	758400.3	749449.9
Model 0	886676.3	877726.0
Model 4	927185.5	918235.2

Table 4: AIC of models for the Barabasi Albert preferential algorithm for vertex arriving at t=100

Model	AIC	$\Delta AIC$
Model 2+	-75363.2	0.0
Model 2	-31236.3	44126.9
Model 1+	-21762.1	53601.1
Model 1	-18909.4	56453.8
Model 4+	132811.5	208174.7
Model 0+	408336.0	483699.2
Model 3+	409360.5	484723.7
Model 3	518236.0	593599.2
Model 0	658658.4	734021.6
Model 4	703537.8	778901.0

Table 5: AIC of models for the Barabasi Albert preferential algorithm for vertex arriving at t=1000

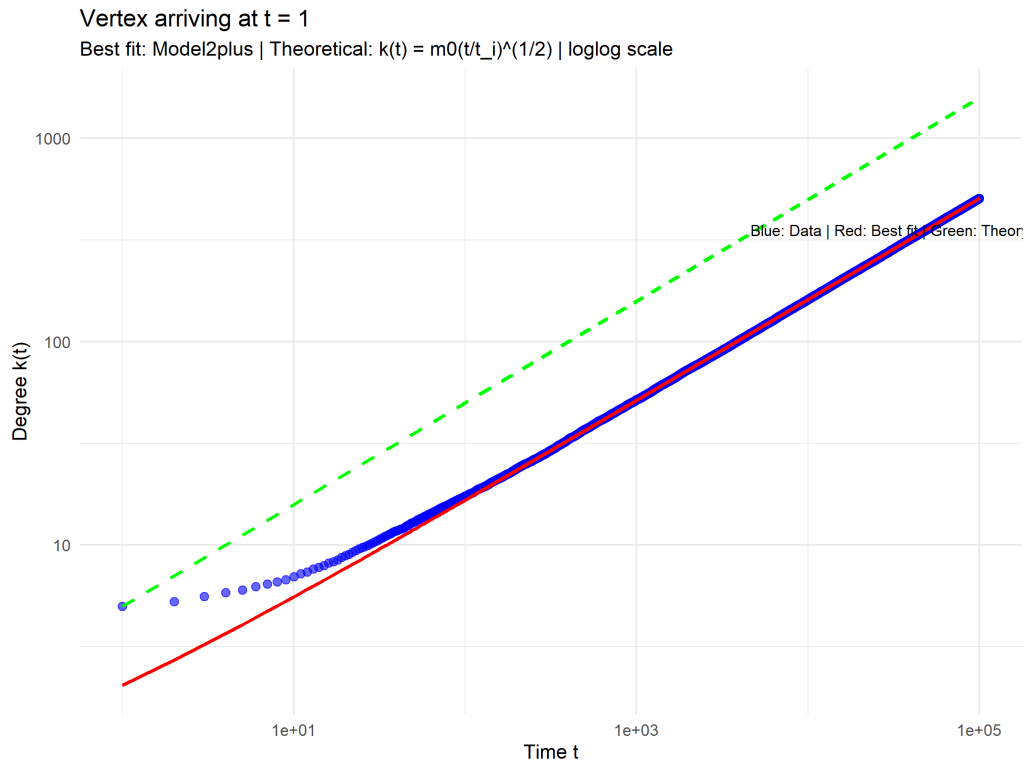


Figure 3: Degree growth of the vertex arriving at  $t = 1$  for BA PA model

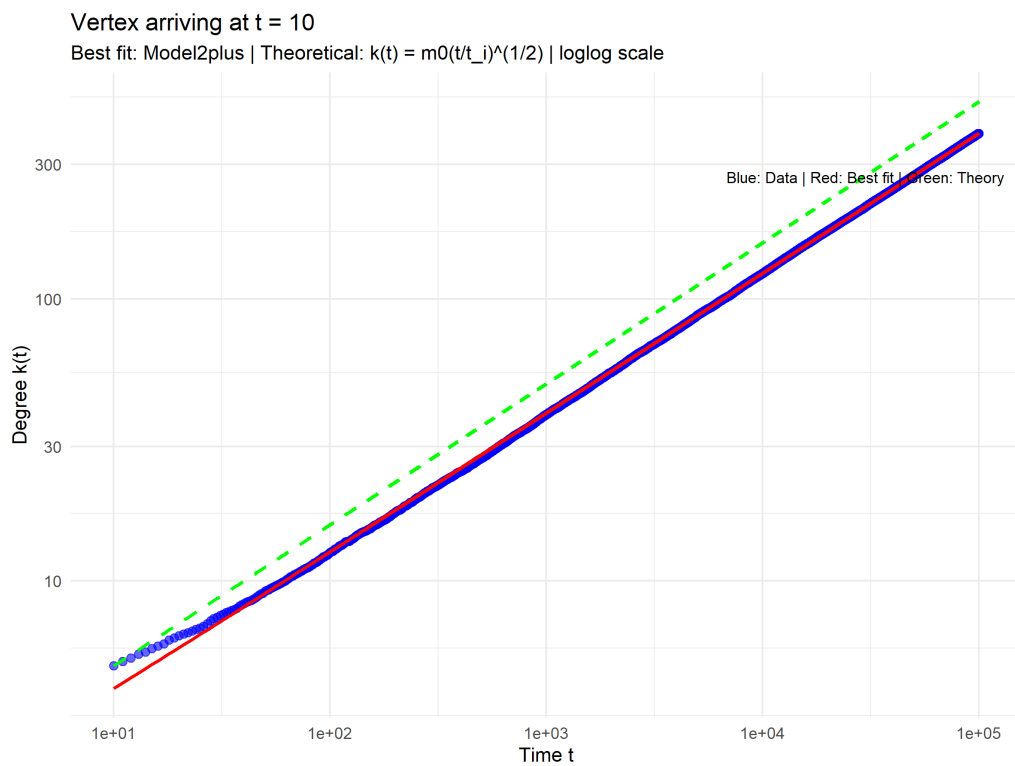


Figure 4: Degree growth of the vertex arriving at  $t = 10$  for BA PA model

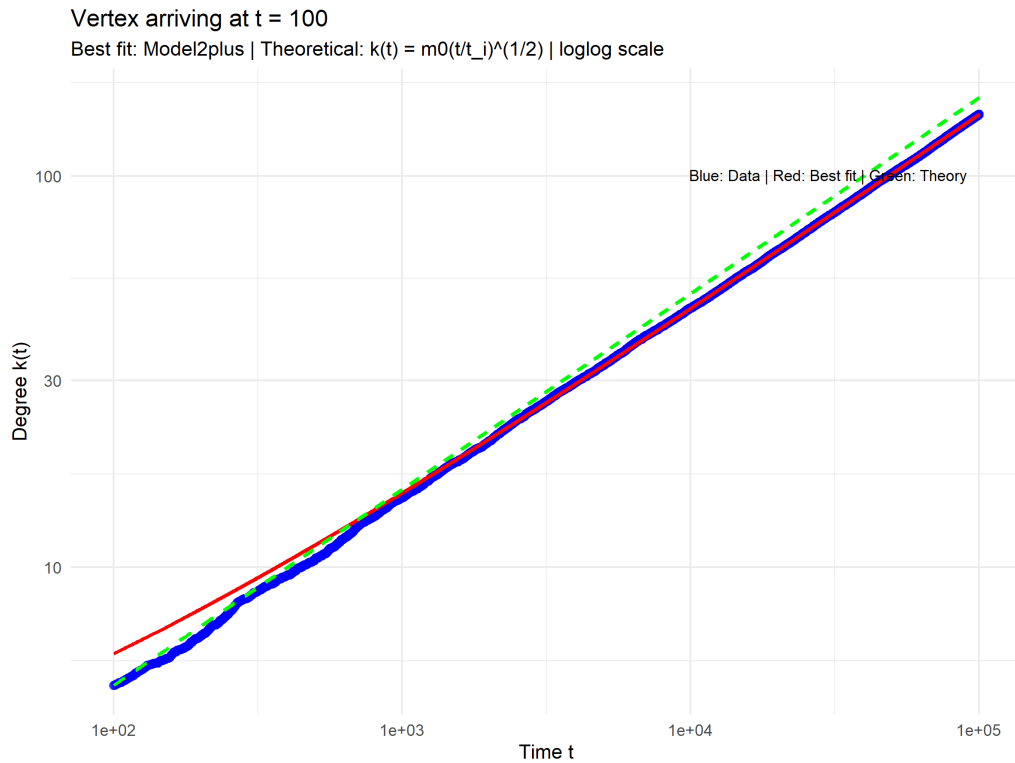


Figure 5: Degree growth of the vertex arriving at  $t = 100$  for BA PA model

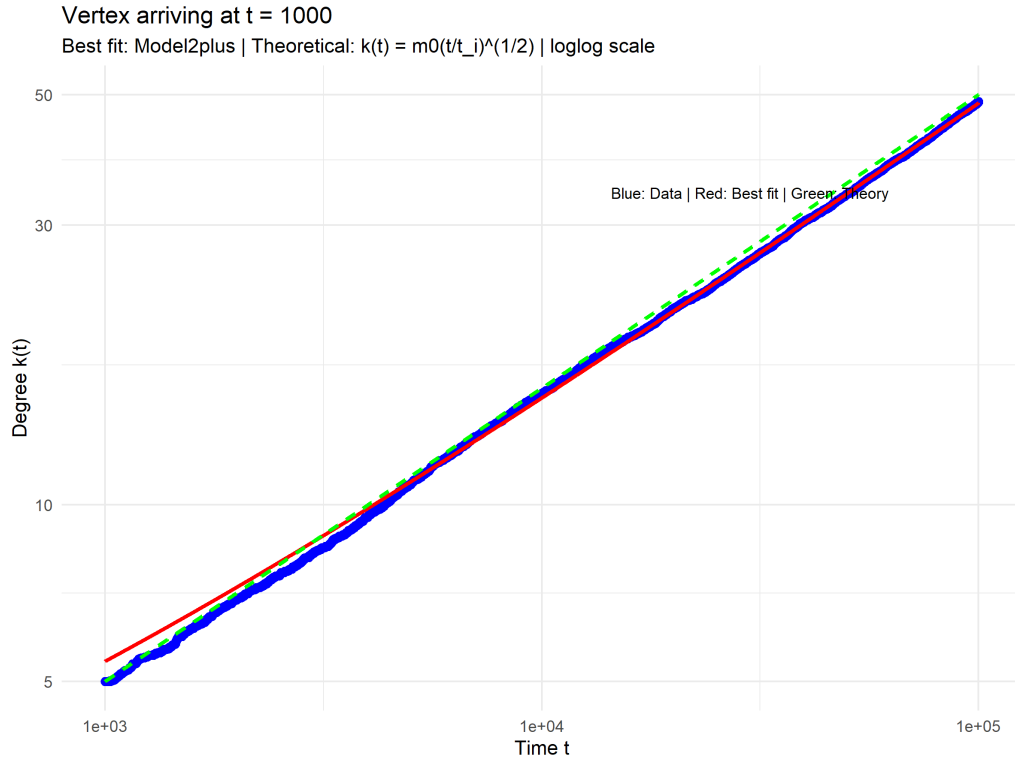


Figure 6: Degree growth of the vertex arriving at  $t = 1000$  for BA PA model

To sum up, we report below the best-fit parameters obtained for the vertices arriving at different times  $t_i$ . For each case the Model 2+ was selected as the best performer.

#### Vertex arriving at $t = 1$

$$a = 1.6395, \quad b = 0.4979, \quad d = 0.4065$$

**Vertex arriving at  $t = 10$** 

$$a = 1.2692, \quad b = 0.4967, \quad d = 0.1795$$

**Vertex arriving at  $t = 100$** 

$$a = 0.4150, \quad b = 0.5066, \quad d = 1.7449$$

**Vertex arriving at  $t = 1000$** 

$$a = 0.1061, \quad b = 0.5295, \quad d = 1.2992$$

## 2.2 Barabási-Albert with Random Attachment

### 2.2.1 Degree sequence

For the BA model with random attachment, we followed the same procedure as above.

The AIC analysis on the aggregated degree sequence identifies the truncated zeta distribution as the best model in terms of AIC, with an estimated exponent

$$\hat{\gamma} \approx 2.48.$$

However, a visual comparison between the empirical degree distribution and the fitted curves on lin-log scales suggests a different picture.

In particular:

- A geometric distribution with parameter  $\hat{q} \approx 0.10$  already yields a visually better fit across most of the support than the truncated zeta selected by AIC.
- An even better visual fit is obtained by a truncated geometric distribution, with an estimated parameter  $\hat{q} \approx 0.1$ . This model captures both the initial decay and part of the tail behaviour more convincingly than the truncated zeta.

Thus, while AIC formally favours the truncated zeta model with  $\hat{\gamma} \approx 2.36$ , the geometric and especially the truncated geometric distributions provide substantially better visual fits. This apparent contradiction is analysed in more detail in the discussion 3.2.1.

Model	AIC	$\Delta\text{AIC}$	Parameters
Zeta Trunc	55625331	0.0	$\gamma = 2.3646, k_{\max} = 80$
Zeta	55956277	330946.6	$\gamma = 2.482$
Geometric	67026455	11401124.1	$q = 0.0909$
Poisson	65454409	9829078.1	$\lambda = 9.9994$
Geom Trunc	67011878	11386547.3	$q = 0.0904, k_{\max} = 80$

Table 6: AIC of models for the Barabási–Albert random algorithm for the degree distribution.

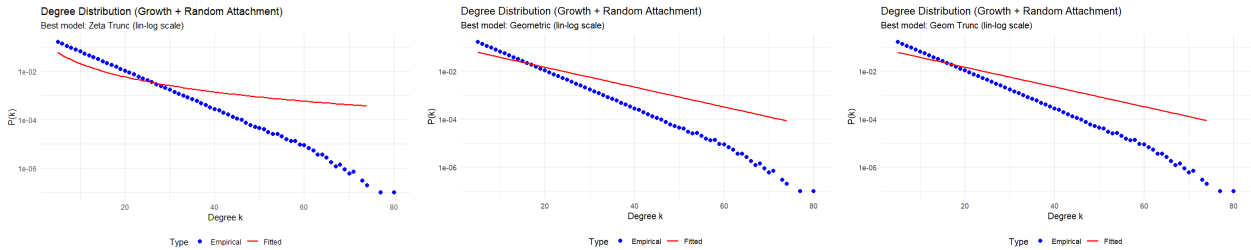


Figure 7: Best degree distribution fit for the BA random model

### 2.2.2 Scaling of vertex degree over time

We plotted the rescaled degree  $k'_i(t)$  obtained by applying the transformation:

$$k''_i(t) = k_i(t) + m_0 \log(n_0 + t_i - 1) - m_0 \approx m_0 \log(m_0 + t - 1).$$

This time we used a log-lin scale was used for the plot to show the log dependency.

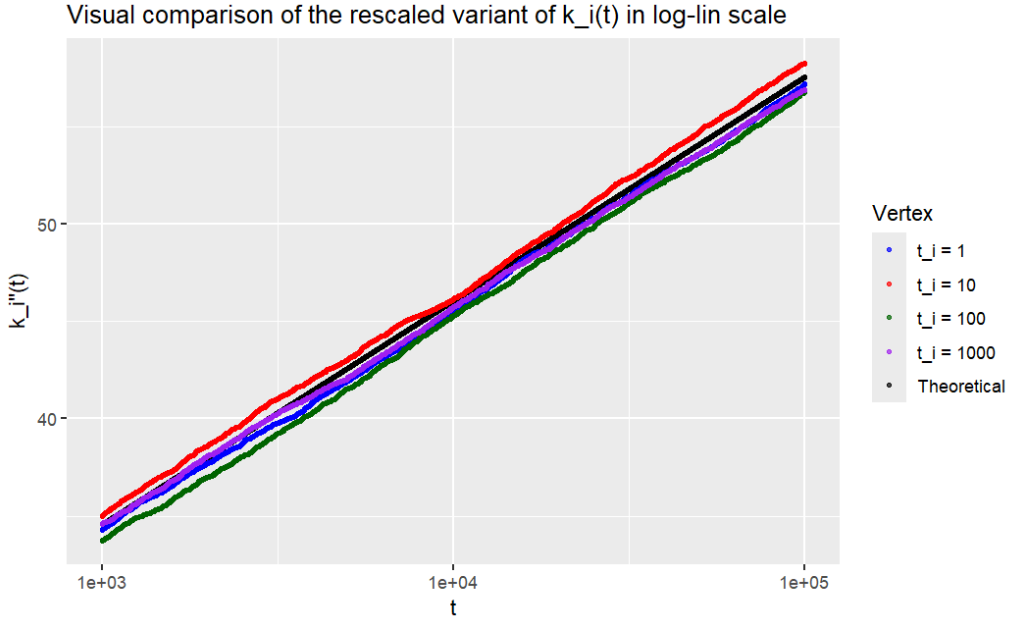


Figure 8: Rescaled variant of degree growth over time for different arrival times

Here we also show the four lin-log plots of the evolution of the degree over time for the vertices arriving at times  $t = 1, t = 10, t = 100$ , and  $t = 1000$ .

The colour legend is the same as the previous plots. This time, the theoretical curve is given by the formula:

$$k_i(t) \approx m_0 (\log(m_0 + t - 1) - \log(n_0 + t_i - 1) + 1)$$

In addition, we present the AIC of the different models and the performance of the fits:

Model	AIC	$\Delta AIC$
Model 4+	-168723.5	0.0
Model 2+	-92274.4	76449.1
Model 2	156461.1	325184.5
Model 4	198104.8	366828.3
Model 1+	384935.3	553658.7
Model 0+	466537.5	635260.9
Model 3+	466627.9	635351.3
Model 3	476794.3	645517.7
Model 1	761642.7	930366.2
Model 0	875180.5	1043904.0

Table 7: AIC of models for the random attachment algorithm for vertex arriving at  $t=1$

Model	AIC	$\Delta AIC$
Model 2+	-189366.8	0.0
Model 4+	-139701.6	49665.1
Model 2	133732.3	323099.1
Model 4	276258.2	465625.0
Model 1+	374756.7	564123.5
Model 0+	462351.1	651717.9
Model 3+	462449.4	651816.2
Model 3	474328.8	663695.6
Model 1	745326.8	934693.6
Model 0	862191.4	1051558.1

Table 8: AIC of models for the random attachment algorithm for vertex arriving at  $t=10$

Model	AIC	$\Delta AIC$
Model 4+	-158439.0	0.0
Model 2+	-76969.8	81469.2
Model 2	190345.3	348784.3
Model 1+	367316.2	525755.2
Model 4	397901.0	556340.0
Model 0+	454345.7	612784.7
Model 3+	454452.7	612891.6
Model 3	468906.7	627345.7
Model 1	668365.2	826804.2
Model 0	798073.8	956512.8

Table 9: AIC of models for the random attachment algorithm for vertex arriving at  $t=100$

Model	AIC	$\Delta AIC$
Model 4+	-257978.6	0.0
Model 2+	-89945.2	168033.5
Model 2	179890.0	437868.6
Model 1+	303112.9	561091.5
Model 0+	402783.6	660762.2
Model 3+	402930.9	660909.5
Model 3	426540.3	684518.9
Model 4	455265.6	713244.2
Model 1	532330.9	790309.5
Model 0	693259.1	951237.8

Table 10: AIC of models for the random attachment algorithm for vertex arriving at  $t=1000$

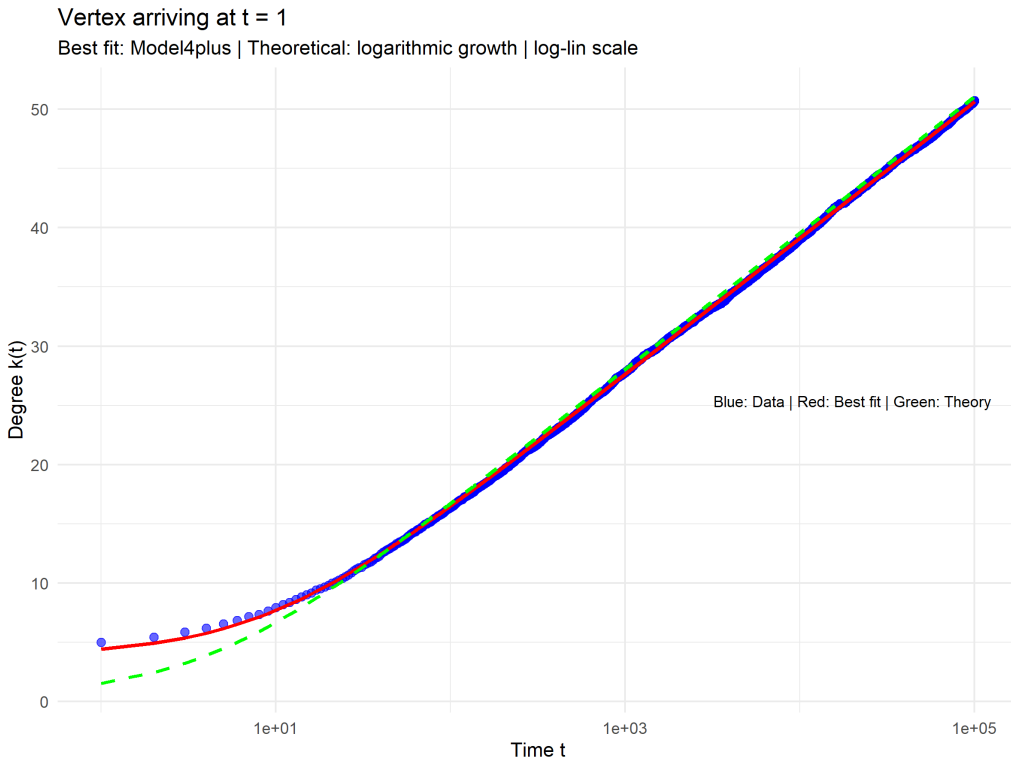


Figure 9: Degree growth of the vertex arriving at  $t = 1$  for BA RA model

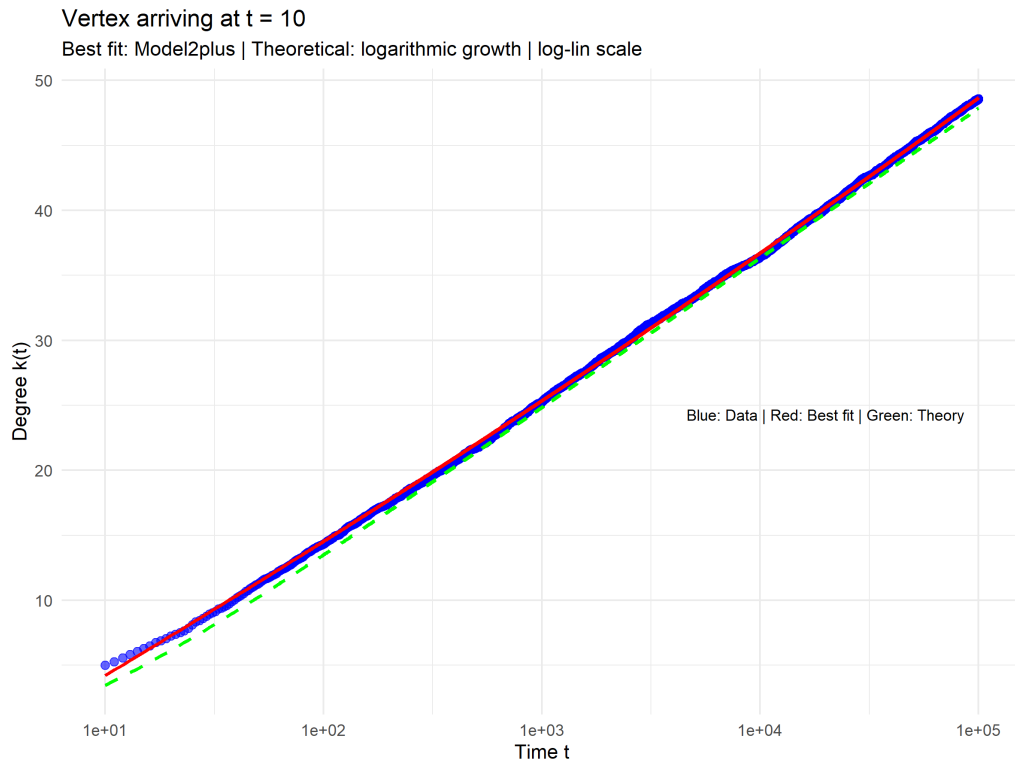


Figure 10: Degree growth of the vertex arriving at  $t = 10$  for BA RA model

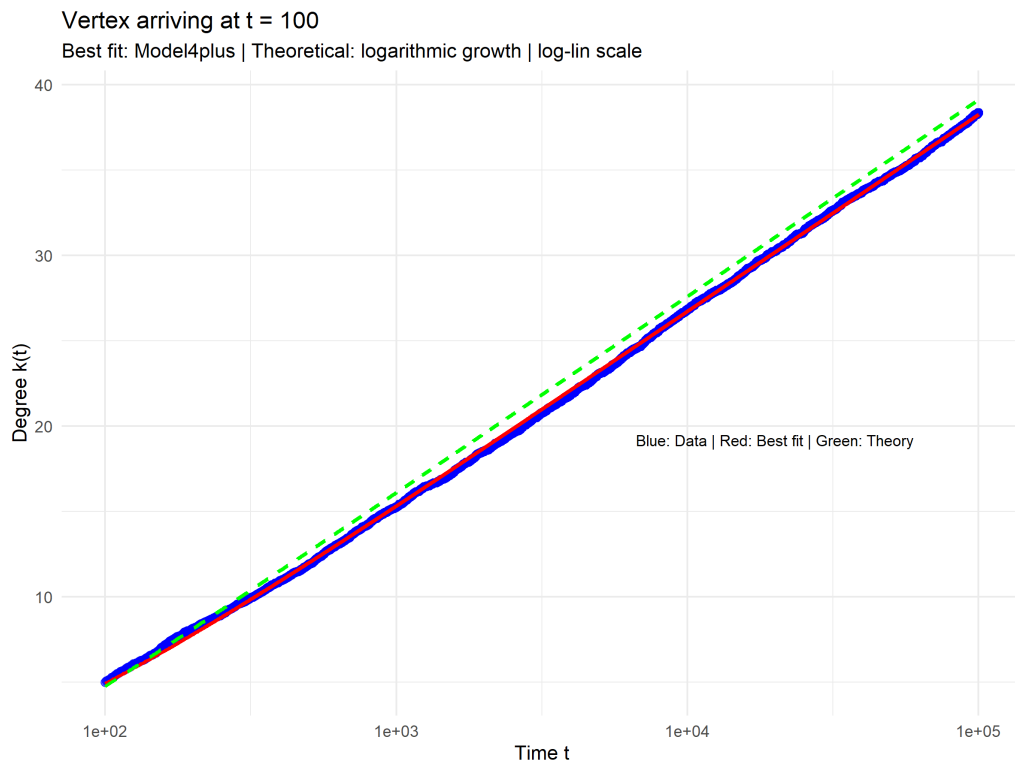


Figure 11: Degree growth of the vertex arriving at  $t = 100$  for BA RA model

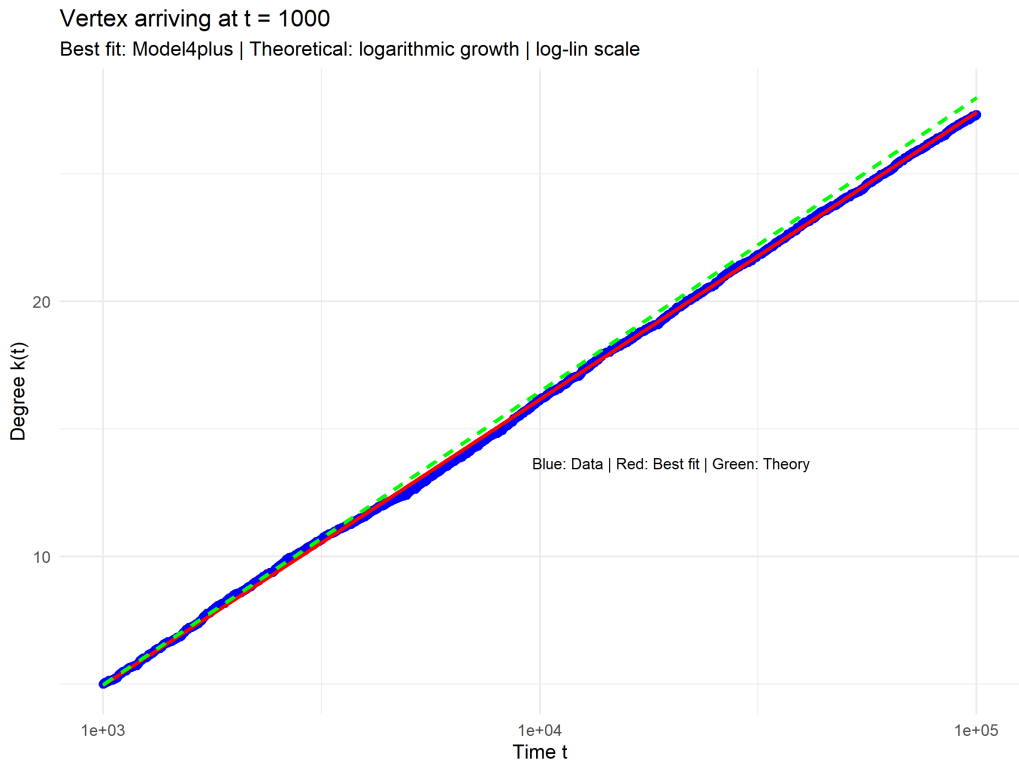


Figure 12: Degree growth of the vertex arriving at  $t = 1000$  for BA RA model

Here, we also report the values of the best model for each degree growth:

**Vertex arriving at  $t = 1$**  Best model: Model4plus

$$a = 5.0008, \quad d_1 = 8.7459, \quad d_2 = -6.9537$$

**Vertex arriving at  $t = 10$**  Best model: Model2plus

$$a = 195.7703, \quad b = 0.0212, \quad d = -201.3539$$

**Vertex arriving at  $t = 100$**  Best model: Model4plus

$$a = 5.0085, \quad d_1 = 29.5907, \quad d_2 = -19.4225$$

**Vertex arriving at  $t = 1000$**  Best model: Model4plus

$$a = 4.8882, \quad d_1 = 10.44, \quad d_2 = -28.8621$$

## 2.3 No-Growth Model with Random Attachment

### 2.3.1 Degree sequence

As before, we ran 100 independent simulations, recorded the final degrees, and aggregated them into a single empirical degree sequence.

We then fitted several candidate distributions and compared them by AIC as before. In this case, both criteria, AIC and visual comparison, clearly indicate that the best fit is provided by a Gaussian distribution.

The Gaussian curve with these parameters follows the empirical histogram very closely, capturing both the central bulk of the distribution and its overall spread.

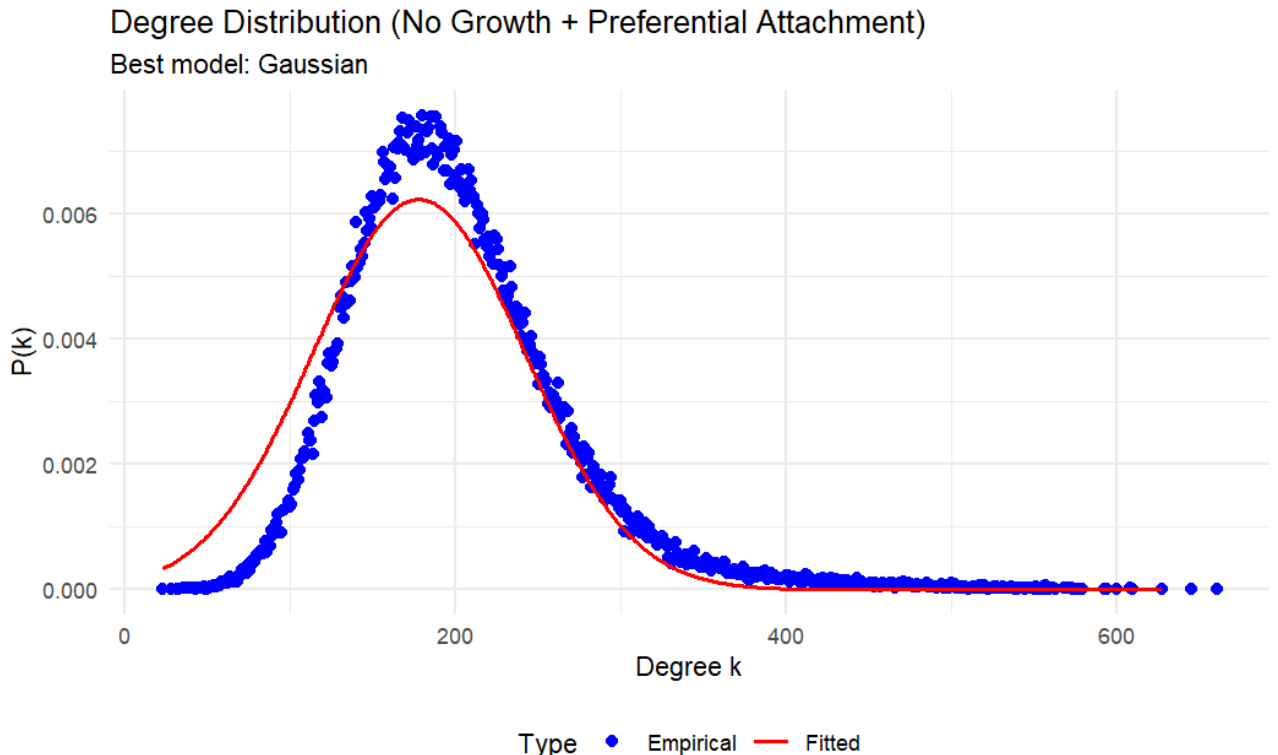


Figure 13: Best degree distribution fit for the No-Growth preferential model

Model	AIC	$\Delta\text{AIC}$	Parameters
Gaussian	1116029	0.0	$\mu = 199.9792, \sigma = 64.1477$
Geometric	1260146	144116.9	$q = 0.005$
Zeta	1383792	267762.9	$\gamma = 1.3119$
Zeta Trunc	1293433	177403.9	$\gamma = 1, k_{\max} = 660$
Geom Trunc	1248377	132348.0	$q = 0.0038, k_{\max} = 660$
Poisson	2655656	1539626.2	$\lambda = 199.9792$

Table 11: AIC of models for the No-Growth preferential algorithm for the degree distribution.

### 2.3.2 Scaling of vertex degree over time

Once again, we analyzed the degree growth over time of four nodes chosen at random. The growth of the degree over time is supposed to follow this theoretical distribution:

$$k_i(t) = \frac{2m_0}{n_0}t$$

To do this, we plotted on the same graphic the theoretical curve (the black line) and the growth of the vertices (the other 4 colours) in a lin-lin plot, to show the linear scaling of the distribution. Here's the result:

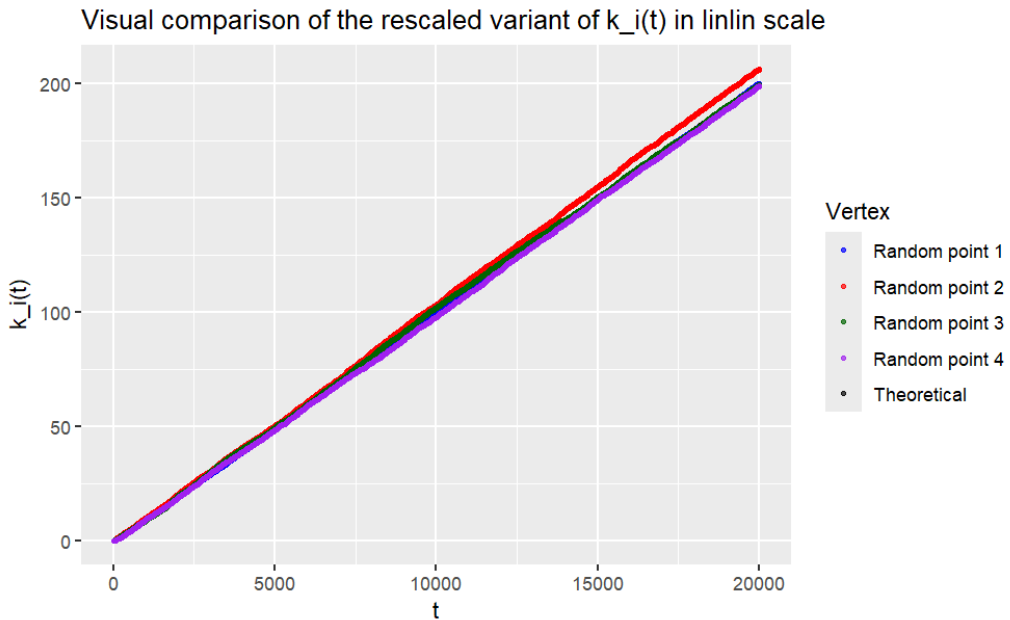


Figure 14: Rescaled variant of degree growth over time for 4 vertices chosen randomly

Now we also present the tables that we used for model selection, the plots of the evolution of the degree over time of those vertices from the beginning until  $t_{max}$  and the comparison with the theoretical curve:

Model	AIC	$\Delta AIC$
Model 2+	8100.1	0.0
Model 0+	8496.7	396.6
Model 2	11780.4	3680.3
Model 3+	21089.6	12989.5
Model 0	24921.9	16821.8
Model 4+	45717.2	37617.1
Model 1+	154929.2	146829.1
Model 3	161941.4	153841.3
Model 1	182856.9	174756.8
Model 4	211934.1	203834.1

Table 12: AIC of models for the no growth model for random vertex 1

Model	AIC	$\Delta AIC$
Model 2+	27428.1	0.0
Model 0+	27824.7	396.6
Model 2	27827.4	399.3
Model 0	32643.9	5215.8
Model 3+	34855.4	7427.4
Model 4+	51556.7	24128.6
Model 1+	156437.8	129009.7
Model 3	163387.9	135959.9
Model 1	184136.4	156708.3
Model 4	213268.5	185840.4

Table 13: AIC of models for the no growth model for random vertex 2

Model	AIC	$\Delta AIC$
Model 4+	36029.4	0.0
Model 2+	39348.7	3319.3
Model 2	47283.9	11254.5
Model 0+	50104.5	14075.1
Model 0	50152.8	14123.3
Model 3+	58810.2	22780.7
Model 1+	153260.0	117230.6
Model 3	163467.6	127438.2
Model 1	182249.1	146219.6
Model 4	211883.3	175853.9

Table 14: AIC of models for the no growth model for random vertex 3

Model	AIC	$\Delta AIC$
Model 2+	13019.0	0.0
Model 2	13727.4	708.4
Model 3+	16143.0	3124.0
Model 0+	21979.2	8960.2
Model 0	42398.1	29379.2
Model 4+	54463.5	41444.5
Model 1+	155422.8	142403.9
Model 3	161486.8	148467.8
Model 1	183037.1	170018.2
Model 4	211836.4	198817.4

Table 15: AIC of models for the no growth model for random vertex 4

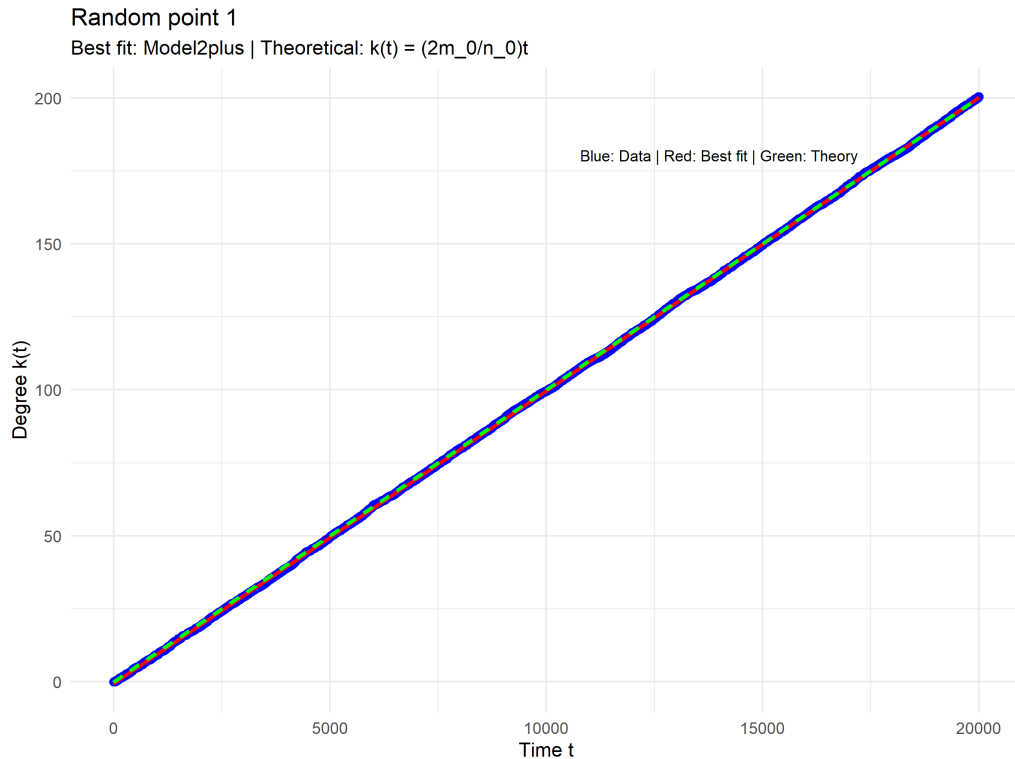


Figure 15: Degree growth of the first vertex for the NG model

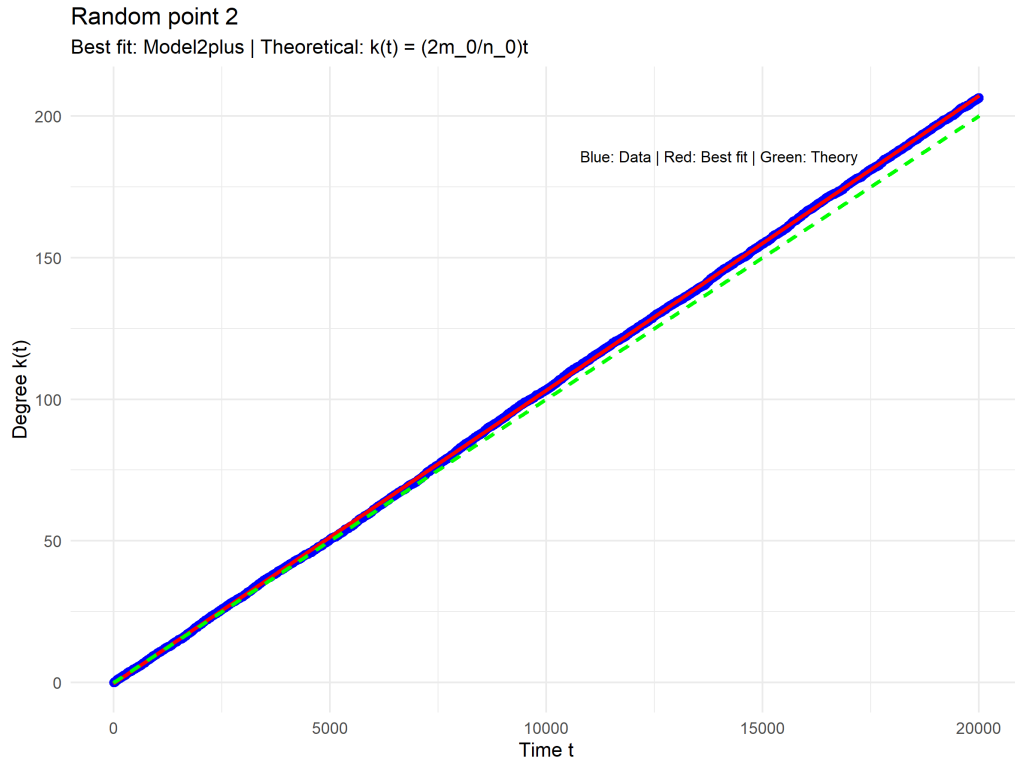


Figure 16: Degree growth of the second vertex for the NG model

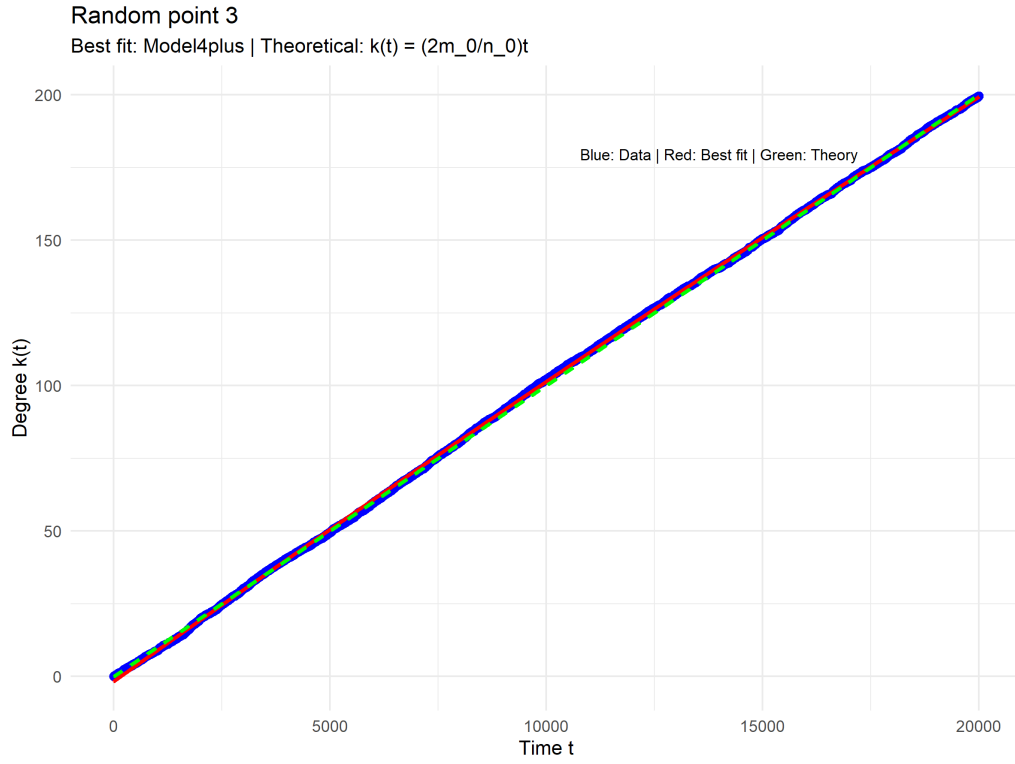


Figure 17: Degree growth of the third vertex for the NG model

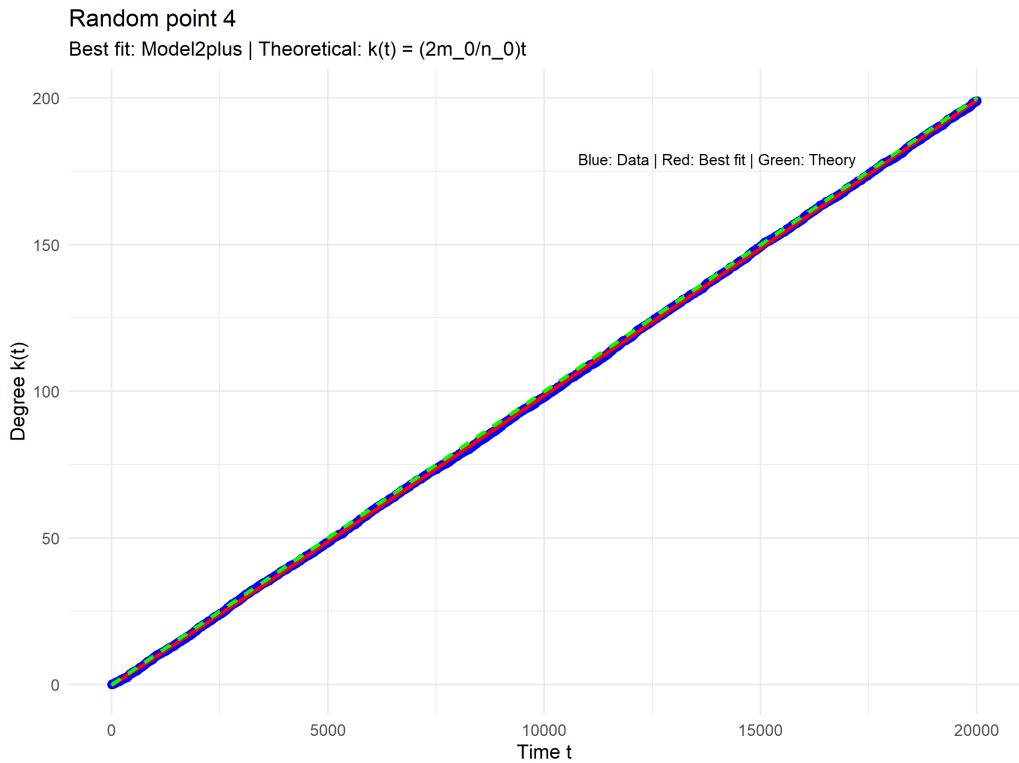


Figure 18: Degree growth of the fourth vertex for the NG model

These are the values of the parameters for the best model according to AIC:

**Random point 1** Best model: Model2plus

$$a = 0.009816, \quad b = 1.002177, \quad d = -0.529935$$

**Random point 2** Best model: Model2plus

$$a = 0.010026, \quad b = 1.003407, \quad d = -0.271611$$

**Random point 3** Best model: Model4plus

$$a = 1941.380963, \quad d_1 = 183412.366056, \quad d_2 = -23530.218191$$

**Random point 4** Best model: Model2plus

$$a = 0.008757, \quad b = 1.013159, \quad d = -0.25132$$

### 3 Discussion

#### 3.1 Expectations of the Growth + Preferential Attachment Model

##### 3.1.1 Expected Degree Distribution

From the theoretical analysis of the Barabási–Albert model [1], one expects the stationary degree distribution to follow an asymptotic power law of the form

$$P(k) \propto k^{-\gamma}$$

with exponent

$$\gamma_{\text{theory}} = 3.$$

In our simulations, the best-fit truncated zeta distribution yields an exponent

$$\hat{\gamma} \approx 2.77,$$

which is reasonably close to the theoretical value  $\gamma = 3$  but still exhibits a noticeable discrepancy.

This difference can be largely attributed to finite-size effects and to the heavy-tailed nature of the power-law distribution. Power laws are characterized by very slow decay in the tail; in other words, very large degrees occur with relatively non-negligible probability. When we aggregate 100 independent realizations of the process, these rare but extreme degrees accumulate across runs, effectively making the empirical tail of the distribution even heavier. As a consequence, the likelihood fit becomes more strongly influenced by a relatively small number of large-degree observations in the tail.

This tail dominance manifests in two ways:

1. The estimated exponent  $\hat{\gamma}$  is slightly smaller than the theoretical value 3, reflecting a heavier effective tail in the aggregated data.
2. The quality of the fit around small degrees (the left part of the distribution) is somewhat degraded: a model chosen to optimally match the heavy tail may underfit or overfit the first few degree values, leading to a visibly poorer alignment in that region.

Overall, however, both the AIC-based selection and the visual inspection confirm that a truncated power-law with exponent close to 3 is fully consistent with the theoretical preferential-attachment scenario.

### 3.1.2 Expected Scaling Degree Over Time

**Analysis of the rescaled degree:** To check the validity of the theory, we plotted the rescaled degree  $k'_i(t) = t_i^{1/2} k_i(t)$  on a log-log scale. Theoretically, if the approximation holds, all curves should collapse onto the same trend line proportional to  $t^{1/2}$ , regardless of when the vertex  $i$  arrived.

The plot confirms the expected power-law behavior, with all curves showing a slope close to 0.5. However, we can clearly see that the agreement with the theoretical prediction depends on the arrival time  $t_i$ . For vertices that arrive later in the process (like  $t_i = 100$  and  $t_i = 1000$ ), the curves overlap almost perfectly with the theoretical black line. In contrast, the curve for the first vertex ( $t_i = 1$ ) remains noticeably lower.

This discrepancy occurs because the continuum theory is a mean-field approximation. It describes the system well when the network is large and the variables can be treated as continuous. However, for the very first nodes introduced at the beginning of the simulation, the discrete nature of the process and initial fluctuations are more significant, leading to a deviation from the idealized average behavior.

**Analysis of the best fit:** To quantitatively verify the nature of the degree evolution, we compared several candidate models using the Akaike Information Criterion (AIC). The analysis consistently identifies Model 2+ as the best-performing model across all time series observed (vertices arriving at  $t_i = 1, 10, 100, 1000$ ).

As defined in the model specifications, Model 2+ corresponds to a power-law relationship of the form  $f(t) = at^b + d$ . Beyond merely selecting this functional form, the fitting process provides a crucial insight: the estimated exponent parameter  $b$  is consistently found to be very close to 0.5. This result is significant because it offers robust statistical confirmation of the theoretical prediction, which states that  $k_i(t) \propto t^{1/2}$ .

This statistical evidence is strongly supported by visual inspection of the plot. It is evident that the best-fit model approximates both the empirical data distribution and the theoretical curve with high accuracy. This dual confirmation (statistical and visual) reinforces the conclusion that the degree growth is governed by the expected power-law dynamics of the preferential attachment model.

## 3.2 Expectations of the Growth + Random Attachment Model

### 3.2.1 Expected Degree Distribution

From the analytical theory of the BA model with purely random attachment, the degree evolution of a given vertex can be described as a simple stochastic process driven by random edge arrivals. In the stationary regime, the degree distribution is expected to converge to a geometric law. In particular, one can show that the degree of a randomly chosen vertex has an approximate geometric distribution with parameter

$$p_{\text{theory}} \approx 1 - e^{-1/m_0},$$

where  $m_0$  is the number of edges that each newly added node brings into the network. In our simulations,  $m_0 = 5$ , hence

$$p_{\text{theory}} \approx 1 - e^{-1/5} \approx 1 - e^{-0.2} \approx 1 - 0.8187 \approx 0.1813.$$

The geometric fits obtained from our data have estimated parameters  $\hat{q}$  of the same order of magnitude (e.g.  $\hat{q} \approx 0.1$  for the non-truncated geometric and for the truncated geometric), confirming that the geometric family is indeed a theoretically well-motivated candidate.

Despite this, the AIC-based selection points to a truncated zeta distribution as the best model. However, when the corresponding fitted curve is compared to the data, the truncated power-law offers a rather poor visual fit: it fails to capture the initial part of the distribution and does not align well with the bulk of the empirical probability mass. In contrast, the theoretically expected geometric fit aligns much better with the empirical distribution, though it still suffers from discrepancies in the tail.

The origin of this discrepancy lies again in the heavy tails observed in the simulated degree sequences. Even in the random-attachment setting, repeated simulations and aggregation of final degrees lead to the presence of relatively large-degree vertices across runs. These large degrees are rare but have a strong influence on the likelihood; thus, models with heavier tails (such as truncated power laws) can gain an advantage in AIC despite fitting the majority of the data less well in a visual sense.

To mitigate this tail-driven bias, we introduced the truncated geometric model, which allows us to effectively down-weight or exclude extremely large degrees by enforcing an upper cutoff  $k_{\max}$ . The truncated geometric yields a significantly improved visual fit over the non-truncated geometric, particularly in the right tail. Nevertheless, it still does not perfectly capture the empirical distribution, as the simulated tails remain unusually heavy and continue to impact the fitting procedure.

A possible way to improve the global fit would be to:

- further aggregate or smooth the final degrees across runs (via binning or averaging), reducing the influence of rare extreme values
- Manually truncate the geometric distribution at a lower cutoff, effectively discarding only the very largest degrees that “contaminate” the tail and distort the fit.

Such truncations would be justified as practical modelling choices, aimed at obtaining a model that better represents the bulk behaviour of the degree distribution rather than its extreme outliers.

### 3.2.2 Expected Scaling Degree Over Time

**Analysis of the rescaled degree:** To verify the scaling behavior under the random attachment mechanism, we examined the evolution of the rescaled degree  $k_i''(t)$ . According to the theoretical derivation, this quantity is expected to follow a logarithmic trend approximately equal to  $m_0 \log(m_0 + t - 1)$ , which should be independent of the specific arrival time  $t_i$  of the vertex.

Visual inspection of the plot confirms this prediction with high accuracy. Unlike the preferential attachment case, where early nodes showed some deviation, here the curves for all vertices (arriving at  $t_i = 1, 10, 100, 1000$ ) are practically identical. The trajectories collapse almost perfectly onto a single curve that aligns well with the theoretical prediction (black line). This uniform behavior demonstrates that, once the appropriate rescaling is applied, the growth dynamics in the random attachment model are remarkably robust and independent of the vertex’s entry time into the network.

**Analysis of the best fit:** We performed a model selection procedure to identify the function that best describes the degree evolution under the random attachment mechanism. We compared the candidate models using the Akaike Information Criterion (AIC). Based on the theoretical derivation, we expect a logarithmic growth of the form  $k_i(t) \approx m_0 \log(t)$ .

For the vertices arriving at  $t_i = 1, 100$ , and  $1000$ , the analysis identifies Model 4+ as the best fit. This model is defined as  $f(t) = a \log(t + d_1) + d_2$ . Examining the fitted parameters for these time series, we find that the pre-factor  $a$  is consistently very close to the theoretical expectation. Specifically, we obtained  $a \approx 5.00$  for  $t_i = 1$ ,  $a \approx 5.01$  for  $t_i = 100$ , and  $a \approx 4.89$  for  $t_i = 1000$ . These values are in excellent agreement with the theoretical prediction  $a \approx m_0$ , where  $m_0 = 5$  in our simulation.

However, the parameter  $d_1$  shows a deviation from the theoretical expectation  $d_1 \approx m_0 - 1 = 4$ . The fitted values ( $d_1 \approx 8.7, 29.6$ , and  $10.4$ ) are consistently higher. This discrepancy is likely a numerical artifact resulting from the inclusion of the additional vertical shift parameter  $d_2$  in Model 4+. In the optimization process,  $d_2$  allows for a vertical translation that can compensate for changes in the horizontal shift  $d_1$ , leading to a degeneracy where the solver converges to a statistically optimal curve where  $d_1$  does not strictly adhere to the theoretical shift  $m_0 - 1$ .

Interestingly, for the vertex arriving at  $t_i = 10$ , the AIC selection favors Model 2+ ( $f(t) = at^b + d$ ). While this might initially suggest a deviation from the logarithmic behavior, a closer inspection of the exponent reveals that  $b \approx 0.02$ . Mathematically, for very small  $b$ , a power law behaves as  $t^b \approx 1 + b \ln(t)$ . Therefore, the selection of Model 2+ with such a negligible exponent essentially confirms the logarithmic nature of the growth, fitting the data with a “quasi-logarithmic” power law that likely captured local fluctuations slightly better than the rigid logarithmic model.

### 3.3 Expectations of the No-Growth + Preferential Attachment Model

#### 3.3.1 Expected Degree Distribution

Theoretical analysis of the no-growth, preferential-attachment model indicates that the degree distribution does not remain stationary but evolves over time. The evolution proceeds through three qualitative regimes:

1. At early times, the degree distribution exhibits a heavy-tailed, approximately power-law behaviour, as the preferential mechanism strongly amplifies initial fluctuations.
2. At intermediate times, the distribution becomes increasingly concentrated around its mean and can be well approximated by a Gaussian (or, more precisely, by a binomial distribution that is itself well approximated by a Gaussian or a Poisson, depending on parameters).
3. At very long times, when the network becomes saturated (most of the possible edges have been added), the degree distribution converges to a degenerate distribution, approaching a Kronecker delta: almost all vertices end up with the same degree.

The time configuration we consider in our simulations lies in this intermediate regime, where a Gaussian (or equivalently a binomial well approximated by a Gaussian) is indeed the theoretically expected shape for the degree distribution. This is precisely what we observe: both the AIC-based model selection and the visual inspection confirm that a Gaussian with parameters

$$\hat{\mu} \approx 199.98, \quad \hat{\sigma} \approx 64.15$$

provides the best description of the empirical data.

It is worth noting, however, that the Gaussian fit is not absolutely perfect. The residual discrepancies can again be traced back to the history of the distribution: the system has evolved from a preceding heavy-tailed, power-law-like phase. As a result, the current degree distribution still have the imprint of that earlier regime in the form of slightly heavy tails. These residuals of power-law behaviour bias the empirical distribution, especially in the extremes, and thus prevent the Gaussian from being an exact match.

Despite this minor mismatch due to the tails, the overall agreement between theory and simulation is very good: for the chosen time horizon, the empirical degree distribution can be well captured by a Gaussian law, and this conclusion is robustly supported both by the AIC criterion and by the visual comparison of the fitted curve.

#### 3.3.2 Expected Scaling Degree Over Time

**Analysis of the degree:** Finally, we analyzed the degree evolution in the "No Growth" model, where the number of nodes remains fixed at  $n_0$  throughout the simulation. In this scenario, the mean-field theory predicts a linear growth of the degree, described by  $k_i(t) \approx \frac{2m_0}{n_0}t$ .

We visualized the degree evolution for four randomly selected vertices. The resulting plot confirms that the theoretical prediction is highly accurate. Crucially, the curves for all four vertices are practically indistinguishable and collapse onto the predicted linear trend.

This uniformity reflects the fundamental symmetry of the no-growth system. Since all vertices are present from the beginning ( $t = 0$ ) and compete for edges under identical conditions, there is no "first-mover advantage" or age-based hierarchy. Consequently, every node in the network grows, on average, at the exact same rate.

**Analysis of the best fit:** Finally, we formally tested the validity of  $k_i(t) \approx \frac{2m_0}{n_0}t$  by performing model selection on the degree evolution of four randomly selected vertices. The theory predicts a linear relationship, which corresponds to Model 0 (or Model 0+). However, the AIC-based selection process identified Model 2+ as the best fit for three vertices and Model 4+ for one vertex.

While this result might seemingly contradict the linear prediction, a deeper analysis of the fitted parameters reveals that the selected models are essentially describing linear growth.

For the vertices where Model 2+ ( $f(t) = at^b + d$ ) was selected, the estimated exponent  $b$  is consistently extremely close to 1 (specifically  $b \approx 1.002, 1.003$ , and  $1.013$ ). Since a power law with an exponent of 1 is a straight line ( $t^1 = t$ ), the model selection algorithm preferred Model 2+ only because the additional flexibility of the parameter  $b$  allowed it to capture minor stochastic fluctuations better than the rigid linear Model 0. Physically, however, the result  $b \approx 1$  is a strong confirmation of the linear scaling predicted by the theory.

For the vertex where Model 4+ ( $f(t) = a \log(t + d_1) + d_2$ ) was selected, the parameter  $d_1$  was found to be remarkably large ( $d_1 \approx 1.8 \times 10^5$ ). Mathematically, for a logarithm function with a very large horizontal shift ( $d_1 \gg t$ ), we can approximate the behavior using the Taylor expansion:

$$\log(t + d_1) = \log\left(d_1 \left(1 + \frac{t}{d_1}\right)\right) = \log(d_1) + \log\left(1 + \frac{t}{d_1}\right) \approx \log(d_1) + \frac{t}{d_1}$$

This approximation shows that when  $d_1$  is very large, the logarithmic curve becomes virtually indistinguishable from a linear function with slope  $a/d_1$  and intercept  $\log(d_1) + d_2$  over the observed range. The model fitting procedure likely converged to this "stretched" logarithm because the extremely low curvature allowed it to mimic a line while fitting local noise slightly better than a pure linear model. Thus, even this result is consistent with the linear growth hypothesis.

### 3.4 Conclusions

In conclusion, the results we obtained are not far from the one that we expected from the theory: oftentimes the model chosen by the AIC criterion was the expected one, while in other cases the chosen model still had parameters that were trying to imitate the behaviour of the expected distribution. The results we obtained therefore are satisfactory and the code is overall well performing.

## 4 Methods

In our experiments, we used the following Python packages for the simulations:

- `Numpy` for fast operations over arrays and random elements handling.
- `Os` for the functioning of the .py files.
- `Parallel` and `delayed` from `joblib` for parallelization of the operations on different available CPU cores.
- `Defaultdict` from `collections` for efficient dictionary management with default values.
- `Matplotlib` for data visualization.

For the data analysis, we used the following R packages:

- `VGAM` for fitting discrete distributions such as the zeta distribution.
- `stats4` for maximum likelihood estimation (MLE) and model selection.
- `ggplot2` for advanced data visualization and plotting.
- `dplyr` for efficient data manipulation and transformation.
- `scales` for axis scaling and formatting in plots.
- `minpack.lm` for non-linear least squares fitting using the Levenberg-Marquardt algorithm.

### 4.1 Barabási–Albert Model (Growth + Preferential Attachment)

The BA model is defined by two parameters: the initial number of nodes  $n_0$  and the number of edges  $m_0$  each new node brings. The simulation starts with a complete graph of  $n_0$  nodes. At each time step  $t$ , a new node is added and connected to  $m_0$  existing nodes. The probability that a new node connects to node  $i$  is proportional to its degree  $k_i$ :

$$P(i) = \frac{k_i}{\sum_j k_j}$$

This implements the preferential attachment mechanism, also known as "rich-get-richer" dynamics. We tracked the degree evolution of selected nodes (those arriving at specified times  $t_i \in \{1, 10, 100, 1000\}$ ) throughout the simulation and recorded the final degree sequence after  $t_{\max}$  time steps. To ensure statistical robustness, we repeated the simulation  $N = 100$  times, storing both the degree sequences and the time series for analysis.

### 4.2 Random Attachment Model (Growth + Random Attachment)

For the random attachment variant, the initial setup is identical to the BA model, but new nodes connect to  $m_0$  existing nodes chosen uniformly at random, i.e.,

$$P(i) = \frac{1}{N(t)}$$

where  $N(t) = n_0 + t$  is the number of existing nodes at time  $t$ . This model serves as a null comparison to preferential attachment, isolating the effect of network growth without the rich-get-richer mechanism. Degree evolution for the same arrival times and final degree sequences were tracked and aggregated over multiple runs using the same parallelization scheme.

### 4.3 No-Growth Preferential Attachment

The no-growth model simulates a fixed-size network of  $n_0$  nodes where, at each time step,  $m_0$  edges are added between nodes according to preferential attachment. No new nodes are introduced. The probability of selecting node  $i$  as the first endpoint of a new edge is:

$$P(i) = \frac{k_i}{\sum_{j=1}^{n_0} k_j}$$

After selecting node  $i$ , the second endpoint  $j$  is chosen with probability proportional to its degree, excluding node  $i$  itself:

$$P(j|i) = \frac{k_j}{\sum_{l \neq i} k_l}$$

We ensured the graph remained simple (no self-loops or duplicate edges) by rejection sampling: if an edge  $(i, j)$  already exists, we resampled  $j$  until a valid pair was found. Degree evolution for four randomly selected nodes was recorded over time, and the final degree sequence was saved after  $t_{\max}$  edge additions. Multiple independent runs were performed to estimate mean behavior and variability.

### 4.4 Data Storage and Preprocessing

Simulation outputs (degree sequences and time series) were saved as plain text files for subsequent analysis in R. For each model and each tracked arrival time  $t_i$ , we stored:

- The mean degree evolution  $\langle k_i(t) \rangle$  averaged over all realizations.
- The standard deviation  $\sigma_{k_i}(t)$  quantifying the variability across runs.
- The concatenated degree sequences from all runs for distribution fitting.

For the growth models, time series were stored starting from the arrival time  $t_i$  of each tracked node. For the no-growth model, degree evolution was tracked for the entire duration starting from  $t = 1$ . Degree sequences were flattened into a single vector for maximum likelihood estimation.

### 4.5 Choice of Parameters

The simulation parameters were chosen to balance computational feasibility with statistical reliability, while ensuring that the networks reach their asymptotic behavior:

- **Initial network size ( $n_0$ ):** Set to  $n_0 = 10$  for growth models (BA preferential and random attachment) and  $n_0 = 1000$  for the no-growth model. For growth models, a small initial network allows clear observation of the transient dynamics and convergence to asymptotic scaling behavior without introducing significant finite-size effects during the early growth phase. The network quickly becomes large compared to  $n_0$  (after  $t \gg n_0$  steps), making the initial condition negligible. For the no-growth model, a larger network is necessary because the total number of nodes remains fixed, and we need a sufficient statistical sample to observe meaningful degree evolution through edge addition alone. With  $n_0 = 1000$  nodes, we can track the degree distribution and evolution of multiple vertices over time without saturating the network too quickly.
- **Number of edges per node ( $m_0$ ):** Fixed at  $m_0 = 5$  for all models. This value ensures sufficient connectivity while maintaining computational efficiency. It is large enough to produce stable degree distributions and clear scaling behavior (avoiding the extreme sparsity regime where  $m_0 = 1$  or  $m_0 = 2$ ), but small enough to avoid saturation effects in finite-time simulations. The average degree in the network grows as  $\langle k \rangle \approx 2m_0 = 10$ , which is a reasonable value for observing power-law and exponential cutoffs.
- **Maximum time ( $t_{\max}$ ):** Set to  $t_{\max} = 100,000$  for growth models and  $t_{\max} = 20,000$  for the no-growth model. These values were selected to ensure convergence of the degree distribution and time series to their asymptotic behavior. For the BA model,  $t_{\max} = 100,000$  ensures that the network contains  $N(t_{\max}) = n_0 + t_{\max} = 100,010$  nodes, which is sufficiently large to observe the power-law tail of the degree distribution extending over multiple decades in a log-log plot. The maximum degree scales as  $k_{\max} \sim m_0 \sqrt{t_{\max}} \approx 1,580$ , providing a wide dynamic range for statistical analysis. For the no-growth model,  $t_{\max} = 20,000$  corresponds to  $m_0 \cdot t_{\max} = 100,000$  edge additions to a network of fixed size  $n_0 = 1000$ , providing a similar total number of attachment events as the growth models and ensuring that the degree distribution reaches a quasi-stationary regime.

- **Number of realizations ( $N$ ):** We performed  $N = 100$  independent runs for each model. This number provides robust statistical estimates (mean and standard deviation) while remaining computationally tractable. The standard error of the mean scales as  $\text{SEM} = \sigma/\sqrt{N}$ , so  $N = 100$  gives a 10% relative error on the standard deviation, which is sufficient for distinguishing between competing models via AIC. Each run was executed with a different random seed to ensure statistical independence.
- **Tracked arrival times:** Nodes arriving at  $t_i \in \{1, 10, 100, 1000\}$  were tracked throughout the simulation. This logarithmic spacing allows us to observe the rescaling behaviour predicted by theory across multiple orders of magnitude in arrival time.

These parameter choices ensure that our simulations capture the relevant dynamical regimes while maintaining computational efficiency and statistical precision. The networks reach sizes and time scales sufficient to observe asymptotic scaling behaviour, validate theoretical predictions, and distinguish between competing models via AIC-based model selection.

## 4.6 Statistical Analysis and Model Selection

### 4.6.1 Degree Distribution Analysis

We fitted several candidate distributions to the degree sequences using maximum likelihood estimation (MLE). The negative log-likelihood functions were minimized using numerical optimization methods implemented in R's `stats4` package (specifically, the `mle` function with the L-BFGS-B method for bounded optimization).

For each distribution, we computed the corrected Akaike Information Criterion (AICc) to account for finite sample sizes:

$$\text{AICc} = -2 \log \mathcal{L} + 2K \frac{N}{N - K - 1}$$

where  $\mathcal{L}$  is the maximum likelihood,  $K$  is the number of fitted parameters, and  $N$  is the sample size (total number of degree observations). For large  $N$ , AICc converges to the standard AIC.

The candidate distributions were:

- **Poisson distribution, Geometric distribution, Zeta (power-law) distribution (with  $\gamma = 3$ ), Truncated zeta distribution** from the Laboratory 2 session.
- **Truncated geometric distribution:**

$$P(k|q, k_{\max}) = \frac{q(1-q)^{k-1}}{1 - (1-q)^{k_{\max}}}, \quad 1 \leq k \leq k_{\max}$$

where  $k_{\max}$  is the maximum observed degree. The negative log-likelihood is:

$$-\log \mathcal{L} = -N \log q - (M - N) \log(1 - q) + N \log(1 - (1 - q)^{k_{\max}})$$

This model was included to better capture the empirical cutoff in finite-size networks.

- **Gaussian distribution:**

$$P(k|\mu, \sigma) = \frac{1}{\sqrt{2\pi}\sigma} \exp\left(-\frac{(k-\mu)^2}{2\sigma^2}\right)$$

Used only for the no-growth model. The negative log-likelihood is:

$$-\log \mathcal{L} = N \log(\sigma\sqrt{2\pi}) + \frac{S}{2\sigma^2}$$

where  $S = \sum_i (k_i - \mu)^2$ . For the Gaussian fit, we used the `optim` function instead of `mle` due to convergence issues with the Hessian calculation.

Model selection was based on  $\Delta\text{AIC} = \text{AIC}_i - \text{AIC}_{\min}$ , where  $\text{AIC}_{\min}$  is the lowest AIC among all candidate models. We selected the model with the lowest AIC as the best theoretical fit.

To visually assess the goodness-of-fit, we produced comparative plots of the empirical degree distribution (computed as  $P_{\text{emp}}(k) = N_k/N$ , where  $N_k$  is the number of nodes with degree  $k$ ) and the fitted probability mass functions for the best model. For the BA model, we used log-log scales to assess power-law behavior; for the random attachment model, we used lin-log scales to assess exponential decay; and for the no-growth model, we used linear scales to assess Gaussian shape.

### 4.6.2 Analysis of Degree Growth

For the time series analysis, we fitted multiple functional forms to the degree evolution  $k_i(t)$  of nodes arriving at times  $t_i \in \{1, 10, 100, 1000\}$ . The candidate models were designed to capture different growth mechanisms predicted by theory:

#### Linear models:

- **Model 0:**  $k(t) = at$  (proportional growth with no intercept, expected for no-growth PA)
- **Model 0+:**  $k(t) = at + d$  (linear with intercept, allowing for initial degree offset)

#### Power-law models:

- **Model 1:**  $k(t) = at^{\frac{1}{2}}$  (square-root growth with fixed exponent  $b = 1/2$ , expected for BA PA)
- **Model 1+:**  $k(t) = at^{\frac{1}{2}} + d$  (square-root with intercept, accounting for initial degree  $d \approx m_0$ )
- **Model 2:**  $k(t) = at^b$  (general power law with free exponent  $b$ )
- **Model 2+:**  $k(t) = at^b + d$  (power law with intercept)

#### Logarithmic models:

- **Model 4:**  $k(t) = a \log(t + d_1)$  (expected for random attachment,  $d_1$  shifts the argument)
- **Model 4+:**  $k(t) = a \log(t + d_1) + d_2$  (logarithmic with additional vertical shift)

#### Exponential models:

- **Model 3:**  $k(t) = ae^{ct}$  (exponential growth, not expected but tested for completeness)
- **Model 3+:**  $k(t) = ae^{ct} + d$  (exponential with intercept)

All models were fitted using non-linear least squares via the Levenberg-Marquardt algorithm implemented in the `minpack.lm` R package (function `nlsLM`). To obtain robust initial parameter estimates and improve convergence, we performed linearized regressions:

- For power-law models:  $\log(k + 1) \sim \log(t)$  provides initial estimates via  $\log(k + 1) \approx \log(a) + b \log(t)$ . We extract  $a = \exp(\beta_0)$  and  $b = \beta_1$  from the linear fit coefficients.
- For exponential models:  $\log(k + 1) \sim t$  provides initial estimates via  $\log(k + 1) \approx \log(a) + ct$ . We extract  $a = \exp(\beta_0)$  and  $c = \beta_1$ .
- For logarithmic models:  $k \sim \log(t)$  provides an initial estimate for  $a = \beta_1$ , with  $d_1$  initialized to 1.
- For linear models: We use standard linear regression (`lm` function).

Model selection was performed using the AIC for non-linear regression:

$$\text{AIC} = n \log(2\pi) + n \log\left(\frac{\text{RSS}}{n}\right) + n + 2(p + 1)$$

where RSS is the residual sum of squares,  $n$  is the number of time points in the series (after filtering for  $t \geq t_i$ ), and  $p$  is the number of fitted parameters.

## References

- [1] Caldarelli, G. (2007). *Scale-Free Networks: Complex Webs in Nature and Technology*. Oxford University Press.